Available online at www.sciencedirect.com
SCIENCE DIRECT®
International Journal of Solids and Structures 42 (2005) 2517–2531
INTERNATIONAL JOURNAL OF SOLIDS and STRUCTURES
www.elsevier.com/locate/ijsolstr

Dynamic response of various von-Kármán non-linear plate models and their 3-D counterparts

Z. Yosibash [a,*], R.M. Kirby [b]

[a] *Pearlstone Center for Aeronautical Engineering Studies, Department of Mechanical Engineering, Ben-Gurion University, P.O. Box 653, Beer-Sheva, 84105, Israel*
[b] *School of Computing, University of Utah, Salt Lake City, Utah 84112, USA*

Received 27 July 2004; received in revised form 6 October 2004
Available online 23 November 2004

Abstract

Dynamic von-Kármán plate models consist of three coupled non-linear, time-dependent partial differential equations. These equations have been recently solved numerically [Kirby, R., Yosibash, Z., 2004. Solution of von-Kármán dynamic non-linear plate equations using a pseudo-spectral method. Comp. Meth. Appl. Mech. Eng. 193 (6–8) 575–599 and Yosibash, Z., Kirby, R., Gottlieb, D., 2004. Pseudo-spectral methods for the solution of the von-Kármán dynamic non-linear plate system. J. Comp. Phys. 200, 432–461] by the Legendre-collocation method in space and the implicit Newmark-β scheme in time, where highly accurate approximations were realized.

Due to their complexity, these equations are often reduced by discarding some of the terms associated with time derivatives which are multiplied by the plate thickness squared (being a small parameter). Because of the non-linearities in the system of equations we herein quantitatively investigate the influence of these a-priori assumption on the solution for different plate thicknesses. As shown, the dynamic solutions of the so called "simplified von-Kármán" system do not differ much from the complete von-Kármán system for thin plates, but may have differences of few percent for plates with thicknesses to length ratio of about 1/20. Nevertheless, when investigating the modeling errors, i.e. the difference between the various von-Kármán models and the fully three-dimensional non-linear elastic plate solution, one realizes that for relatively thin plates (thickness is 1/20 of other typical dimensions), this difference is much larger. This implies that the simplified von-Kármán plate model used frequently in the literature is as good as an approximation as the complete (and more complicated) model. As a side note, it is shown that the dynamic response of any of the von-Kármán plate models, is completely different compared to the linearized plate model of Kirchhoff–Love for deflections of an order of magnitude as the plate thickness.

Keywords: Von-Kármán plate model; Modeling errors; Finite elements; Modal analysis

* Corresponding author. Tel.: +972 8 6477103; fax: +972 8 6477101.
E-mail addresses: zohary@bgu.ac.il (Z. Yosibash), kirby@cs.utah.edu (R.M. Kirby).

0020-7683/$ - see front matter © 2004 Elsevier Ltd. All rights reserved.
doi:10.1016/j.ijsolstr.2004.10.006

1. Introduction

The von-Kármán system is aimed at approximating a plate model (a three-dimensional entity having one of its dimensions much smaller compared to the other two) through a two-dimensional formulation and involves a system of three non-linear time dependent partial differential equations. As the transverse displacement (deflection) in thin plates may be of the same order of magnitude as the plate thickness, the problem is formulated so to account for large strains/deflections in the transverse direction. This system is mathematically and numerically very challenging, so that most previous investigations addressed either the time *independent* system, see e.g. the two books Chia (1980) and Ciarlet (1990) and the references therein, or the eigen-frequencies, see e.g. Han and Petyt (1997). In many practical engineering applications, such as the fluid-structure interaction of a plate embedded in a flow-field, dynamic solutions to the von-Kármán plate equations are required. For example, a three-dimensional aeroelastic solver for non-linear panel flutter, in which the thin plate is represented by the dynamic simplified von-Kármán system is considered in Gordnier and Fithen (2001) and Gordnier and Visbal (2002).

However, due to the complexity of the complete von-Kármán system of equations, explicit solutions prior to Kirby and Yosibash (2004) and Yosibash et al. (2004) are available only for the simplified von-Kármán system, i.e. neglecting *a priori* terms involving in-plane time derivatives and rotational inertia terms. This simplified system was previous considered by Nath and Kumar (1995) (using Chebyshev series), as well as by Gordnier and Fithen (2001) and Gordnier and Visbal (2002) (using finite differences and C^1 h-version finite element methods). The neglected terms are these which are multiplied by the plate thickness, therefore are much smaller in magnitude compared to the other terms in the equations. Also, by neglecting these terms, it implies that the solution is thickness independent. Because the system is non-linear and no study exists which quantifies the influence of the neglected terms on the solution, we herein retain these terms and quantify their influence. A squared plate with hard-clamped boundary conditions is considered, although other boundary conditions can be easily treated.

From the mathematical viewpoint, the complete von-Kármán system (i.e. the system containing rotational ineria terms) has been shown to be well-posed, admitting a unique solution (bounded for all times), see e.g. Lasiecka (1998) and Koch and Lasiecka (2002). The currently available proofs of well-posedness require the inclusion of the rotational inertia terms. At this time, the authors are not aware of results which prove well-posedness for simplifications of the von-Kármán system (although commonly used in practice).

In view of the mathematical complexity of the von-Kármán plate model, namely, being a set of three coupled non-linear PDEs involving a biharmonic operator, a Laplace operator on acceleration terms and first and second time derivatives, the numerical schemes for solving the problem are complex and documented elsewhere (see Kirby and Yosibash, 2004; Yosibash et al., 2004). Having developed these and verifying the numerical solutions against several analytical ones, and after conducting convergence analyses for the verification of the numerical errors, we use the schemes herein for the following:

- Presenting for the first time the dynamic solution to the complete von-Kármán system (in the past the simplified and full von-Kármán system have been addressed).
- Quantifying the idealization error in dynamic solutions introduced by discarding the inertial terms in the momentum equations for the in-plane displacements, and the angular inertial term in the transverse momentum equation.
- Comparing the solutions of the various von-Kármán models to the three-dimensional solutions, thus enabling a quantitative analysis for small, yet finite plate thicknesses.

The notations, and non-dimensionalization of the various von-Kármán systems (denoted by *simplified*, *full* and *complete*) are presented in Section 2. We also present (for the sake of completeness) a very short summary of the numerical methods used and verified in Kirby and Yosibash (2004) and Yosibash et al.

(2004), namely, the spatial discretization by means of the pseudo-spectral Legendre-collocation method in conjunction with a temporal discretization using the Newmark-β scheme. In Section 3 the differences between the various von-Kármán models for various plate thicknesses, loadings, and values of structural damping coefficient are presented. The differences are due to the various terms neglected in the complete von-Kármán system.

We then address the difference between the von-Kármán model and its linearized counterpart, the Kirchhoff–Love plate model. Although the difference between the *static response* of the von-Kármán plate model and the Kirchhoff–Love plate model is known and documented, the dynamic response difference has not been well-investigated. Taking as an example the non-damped plate under a Heaviside constant load, we show that not only that there is a large difference in the deflection amplitude, but there is also a large difference in the frequency.

Finally, in Section 4 we obtain a fully three-dimensional solution to a non-damped, non-linear elastic plate, under a Heaviside constant load, and investigate the modeling errors of the various von-Kármán plate models. The summary and conclusions are provided in Section 5.

2. Notations and problem formulation

Consider a three-dimensional square plate made of an isotropic elastic material of dimensions $a^* \times a^* \times h^*$, (quantities denoted by asterisk, *, are dimensional quantities which have a non-dimensionalized counterpart), with one of its dimensions h^*, much smaller compared to the other two, i.e. $h^* \ll a^*$. Let us denote the mid-plane surface by $\Omega^* = [0, a^*] \times [0, a^*] \in \mathbb{R}^2$. The Cartesian coordinate system is denoted by $\boldsymbol{x}^* = (x_1^* x_2^* x_3^*)^{\mathrm{T}}$, where the plate thickness is in the x_3^* direction (see Fig. 1).

Let E^*, ν, c^*, ρ^* denote the Young modulus, Poisson ratio, structural viscosity coefficient and density of the plate's material. We assume no body forces are applied on the plate, and on its upper and lower surfaces, traction loading in the x_3^* direction $g_3^{*\pm\frac{h^*}{2}}$ is applied. These are of course prescribed functions of x_1^*, x_2^* and t^* alone.

Following Chia (1980), Lagnese (1989) and Ciarlet (1990), let $\boldsymbol{U}^*(\boldsymbol{x}^*)$ denote the displacement vector $(U_1^* U_2^* U_3^*)^{\mathrm{T}}$ in the corresponding directions, and $\boldsymbol{u}^*(x_1^*, x_2^*, t^*) = (u^* v^* w^*)^{\mathrm{T}}$ denote the mid-plane displacement vector (the deflection of the mid-surface of the plate is w^*).

Due to the difficulties involved in solving the set of three time-dependent (large-deformations) non-linear elasticity equations in a 3-D domain, the dimensional reduced von-Kármán plate model has been considered. It is an approximation of the three-dimensional elastic equations for thin plates, and is derived by

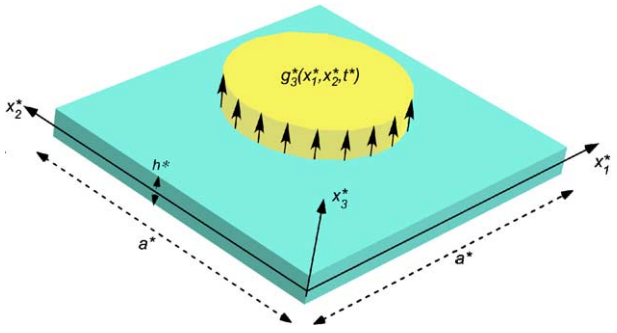

Fig. 1. Notations for plate of interest.

asymptotic analysis. The following assumptions are posted in the asymptotic analysis when deriving the von-Kármán model:

- The displacements $\boldsymbol{U}^*$ are typically of Kirchhoff–Love type, i.e. can be generated from the mid-surface displacement vector as follows:
$$U_1^* = u^* - x_3^* \partial_1 w^*, \quad U_2^* = v^* - x_3^* \partial_2 w^*, \quad U_3^* = w^* \tag{1}$$
where $\partial_i \equiv \frac{\partial}{\partial x_i}$. This is the first source of idealization errors, namely the assumptions on the functional representation of the displacement fields in the x_3^* direction.
- Only the terms involving w^* are retained in the quadratic terms which represent the finite strains.
- The body forces are of the form $\boldsymbol{f} = (0\ 0\ f_3^*)^{\mathrm{T}}$.
- Shear stresses on $x_3^* = \pm h^*/2$ are negligible.

The von-Kármán equations have to be complimented by appropriate boundary conditions. We consider herein hard-clamped boundary conditions:

$$U_1^* = U_2^* = U_3^* = 0 \quad \text{on } \partial\Omega \times \left[-\frac{h^*}{2}, \frac{h^*}{2}\right] \tag{2}$$

which imply the following boundary conditions for the functions u^*,v^*,w^*:

$$u^* = v^* = w^* = \partial_n w^* = 0 \quad \text{on } \partial\Omega \tag{3}$$

The complete von-Kármán set of equations in terms of the three displacement functions u^* is given on $\Omega^* \in \mathbb{R}^2$ by

$$\begin{aligned} &h^*(\rho^* \ddot{w}^* + c^* \dot{w}^*) - \rho^* \frac{(h^*)^3}{12} \Delta^* \ddot{w}^* + D^* (\Delta^*)^2 w^* - \frac{12 D^*}{(h^*)^2} \left[\left(u_{,1}^* + \frac{1}{2} {w_{,1}^*}^2 \right) (w_{,11}^* + \nu w_{,22}^*) \right. \\ &\left. + \left(v_{,2}^* + \frac{1}{2} {w_{,2}^*}^2 \right) (w_{,22}^* + \nu w_{,11}^*) + (1-\nu) \times (v_{,1}^* + u_{,2}^* + w_{,1}^* w_{,2}^*) w_{,12}^* \right] \\ &= {g^*}_3^{\frac{h^*}{2}} + {g^*}_3^{-\frac{h^*}{2}} \stackrel{\text{def}}{=} g^*(x_1^*, x_2^*, t^*) \end{aligned} \tag{4}$$

$$\begin{aligned} &h^*(\rho^* \ddot{u}^* + c^* \dot{u}^*) - \frac{6 D^*}{(h^*)^2} \left(2u_{,11}^* + (1+\nu) v_{,12}^* + (1-\nu) u_{,22}^* \right. \\ &\left. + \left[2 w_{,1}^* w_{,11}^* + (1+\nu) w_{,2}^* w_{,12}^* + (1-\nu) w_{,1}^* w_{,22}^* \right] \right) = 0 \end{aligned} \tag{5}$$

$$\begin{aligned} &h^*(\rho^* \ddot{v}^* + c^* \dot{v}^*) - \frac{6 D^*}{(h^*)^2} \left(2v_{,22}^* + (1+\nu) u_{,12}^* + (1-\nu) v_{,11}^* \right. \\ &\left. + \left[2 w_{,2}^* w_{,22}^* + (1+\nu) w_{,1}^* w_{,12}^* + (1-\nu) w_{,2}^* w_{,11}^* \right] \right) = 0 \end{aligned} \tag{6}$$

where $\bullet_{,i} \equiv \frac{\partial \bullet}{\partial x_i}$, $D^* \stackrel{\text{def}}{=} \frac{E^* (h^*)^3}{12(1-\nu^2)}$ is the flexural rigidity, and Δ^* is the Laplace operator in the plane x_1^*, x_2^*.

Remark 1. One has to find three unknown functions $u^*(x_1^*, x_2^*, t^*), v^*(x_1^*, x_2^*, t^*), w^*(x_1^*, x_2^*, t^*)$, over the two-dimensional domain Ω^*, which describe the displacements of the mid-surface of the plate.

Remark 2. The second term in (4) representing rotational inertia is frequently neglected as well as the first two terms in (5) and (6). Some of the terms in the square brackets are the non-linear terms in the formulation since these involve higher order terms, and also generate the coupling between the various unknown functions. Observe that this is the reason why one cannot split the expression for the energy into pure bending energy and pure tension energy!

2.1. Non-dimensionalization of (4)–(6)

Following Nath and Kumar (1995) we perform the following change of variables:

$$u=\frac{(a^*/2)u^*}{(h^*)^2},\quad v=\frac{(a^*/2)v^*}{(h^*)^2},\quad w=\frac{w^*}{(h^*)},\quad x_1=\frac{x_1^*}{(a^*/2)},\quad x_2=\frac{x_2^*}{(a^*/2)},\quad t=t^*\sqrt{\frac{D^*}{\rho^* h^* (a^*/2)^4}}$$
$$g=\frac{g^*(a^*/2)^4}{D^* h^*},\quad h=\frac{h^*}{(a^*/2)},\quad c=c^*\sqrt{\frac{(a^*/2)^4 h^*}{\rho^* D^*}}$$

With the above set of non-dimensional variables, the *complete* non-dimensional von-Kármán system over a quadrilateral domain $\Omega=[0,2]\times[0,2]$ is given by the following three coupled equations:

$$w_{,tt}+cw_{,t}-\frac{h^2}{12}\Delta w_{,tt}+\Delta^2 w - 12\left[\left(u_{,1}+\frac{1}{2}w_{,1}^2\right)(w_{,11}+vw_{,22})+\left(v_{,2}+\frac{1}{2}w_{,2}^2\right)(w_{,22}+vw_{,11})+(1-v)(v_{,1}+u_{,2}+w_{,1}w_{,2})w_{,12}\right]=g_3 \tag{7}$$

$$\frac{h^2}{6}(u_{,tt}+cu_{,t})-[2u_{,11}+(1+v)v_{,12}+(1-v)u_{,22}+2w_{,1}w_{,11}+(1+v)w_{,2}w_{,12}+(1-v)w_{,1}w_{,22}]=0 \tag{8}$$

$$\frac{h^2}{6}(v_{,tt}+cv_{,t})-[2v_{,22}+(1+v)u_{,12}+(1-v)v_{,11}+2w_{,2}w_{,22}+(1+v)w_{,1}w_{,12}+(1-v)w_{,2}w_{,11}]=0 \tag{9}$$

The system is accompanied by Dirichlet boundary conditions (denoted by "hard clamped") which are:

$$u=v=w=\partial_n w=0\quad \text{on } \partial\Omega \tag{10}$$

Remark 3. The third term in (7) (rotational inertia term) and the first two time dependent terms in ((8) and (9)) are of order h^2 compared to the order one terms in the rest of the equations, and so are commonly neglected (see Chia (1980); Nath and Kumar (1995); Gordnier and Visbal (2002), for example). This set of equations will be denoted as the *simplified von-Kármán* system.

The simplified von-Kármán system contains one prognostic equation (including time derivatives), with two constrain equations, which are time independent. Thus numerical treatment of the simplified system is well-behaved and simple. Nath and Kumar [1] Nath and Kumar (1995) and Gordnier and Visbal (2002) considered the simplified von-Kármán system of equations.

Remark 4. For ease of referencing in the sequel, we denote by *full von-Kármán* system the one obtained when neglecting only the rotational inertia term in (7), but retaining all terms in ((8) and (9)). The set of equations (7)–(9), when all terms are retained is denoted by *complete von-Kármán* system.

2.2. A short summary on the numerical methods for the solution of the von-Kármán system

A detailed analysis of the numerical methods and their convergence properties for the full and simplified von-Kármán models is provided in Kirby and Yosibash (2004) and Yosibash et al. (2004), and this subsection is a short summary for the sake of self consistency of the paper.

[1] Notice that Nath and Kumar (1995) has an error in Eqs. (1) and (B.1), where instead of $(1-v)$ it mistakenly has $(1-v^2)$. Furthermore, the non-dimensionalization of the viscosity term in Eq. (4) has an error, and ρ should be in the denominator instead of the numerator.

We use the Legendre collocation method Canuto et al. (1987) and Trefethen (2000) for the spatial discretization and the Newmark-β scheme Humar (2002) for integration in time. In the Legendre collocation method, each of the unknown functions u,v,w at each time step are approximated by a polynomial of the form (here we show w's approximation):

$$w_M(x_1,x_2)=\sum_{i=0}^{M}\sum_{j=0}^{M} w((x_1)_i,(x_2)_j)h_i(x_1)h_j(x_2) \tag{11}$$

where $h_i((x_1)_k)=\delta_{ik}$ denotes the ith Lagrange interpolating polynomial based upon the Gauss-Lobatto-Legendre point set $\{(x_1)_k\}$ ($h_j((x_2)_k)$) is similarly defined). The coefficients $w((x_1)_i,(x_2)_j)$ are the unknowns which after being found determine the numerical approximation. M denotes the polynomial order per direction given $N=M+1$ collocation points. The exponential convergence properties with increasing N of this methodology were demonstrated in Kirby and Yosibash (2004) for the von-Kármán system, and all von-Kármán simulations presented in the sequel use 13×13 points (a 12th order polynomial in each direction) to represent the solution variables. This order has been shown to produce very accurate solutions for the problems of current interest. Discrete differential operators can be devised based upon derivatives of the Lagrange polynomials; homogeneous Dirichlet boundary conditions are incorporated strongly by adjusting the discrete differential operators. Spatial derivative operators are replaced by the appropriate discrete collocation derivative operators and the non-linearities are handled by point-wise evaluation at the collocation points.

To discretize the von-Kármán system in time, we have chosen to employ the average acceleration variant of the Newmark-β scheme Humar (2002) (with Newmark parameters $\gamma=\frac{1}{2}$ and $\beta=\frac{1}{4}$) which exhibits second-order convergence in time and is unconditionally stable under linear analysis. The Newmark scheme

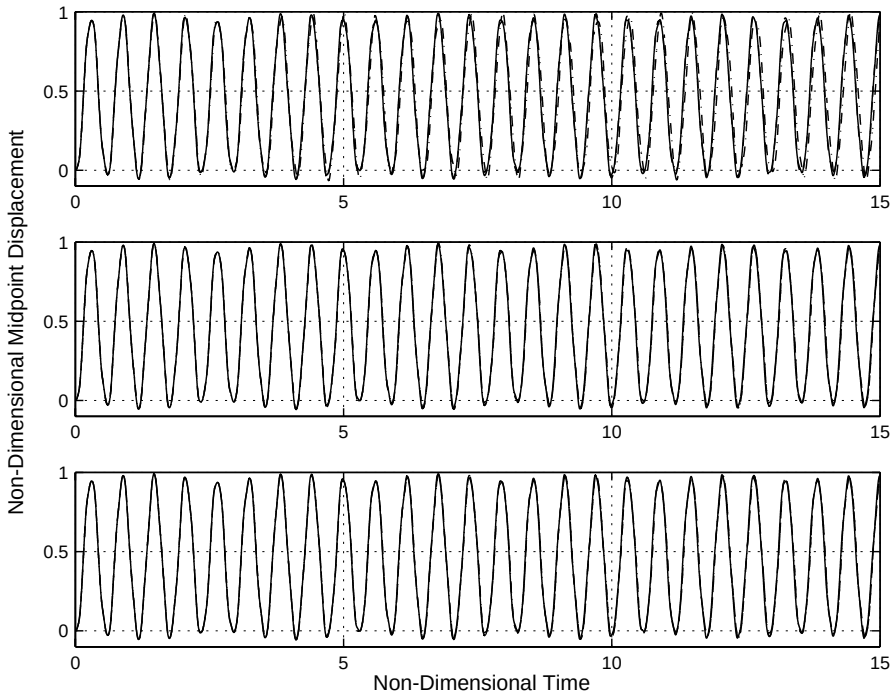

Fig. 2. Constant loading on a non-damped plate: mid-point deflection $w(1,1,t)$ for the simplified (solid line), full (dashed line) and complete (dash-dot line) von-Kármán models. Upper $h=0.1$, middle $h=0.01$ and bottom $h=0.001$ plate.

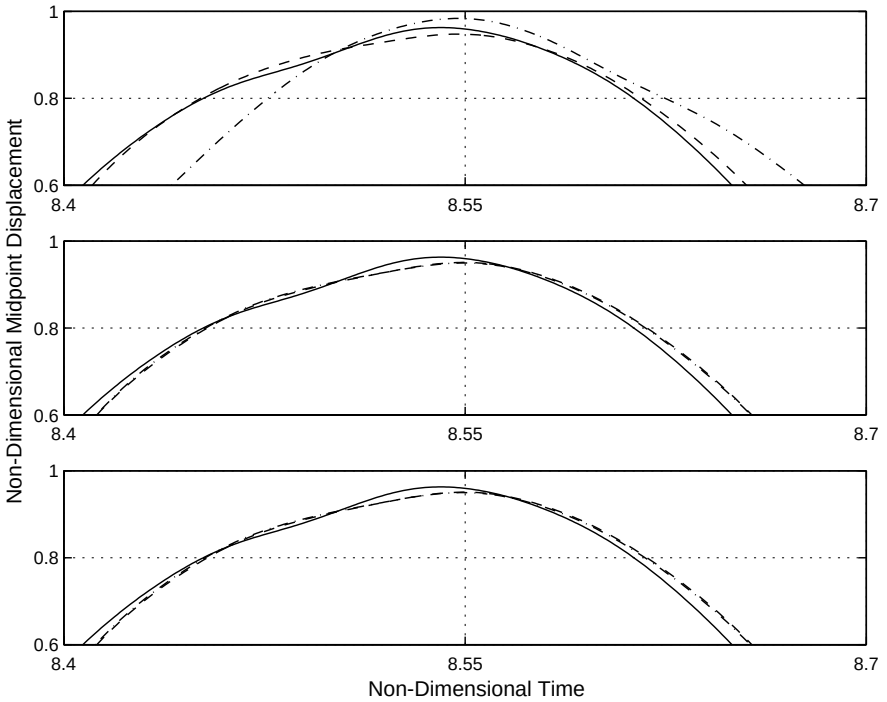

Fig. 3. A zoomed view of Fig. 2 of $w(1,1,t)$ around $t = 8.55$ for the simplified (solid line), full (dashed line) and complete (dash-dot line) von-Kármán models. Upper $h = 0.1$, middle $h = 0.01$ and bottom $h = 0.001$ plate.

requires the implicit evaluation of both the linear and non-linear spatial terms. As in Kirby and Yosibash (2004) and Yosibash et al. (2004), a fixed-point iteration was used (with iteration tolerance of 10^{-10}) to accomplish the necessary implicit solve. For all von-Kármán simulations presented herein, a time step of $\Delta t = 10^{-7}$ was used.

Although the complete von-Kármán system has not been documented elsewhere, its numerical solution is similar to the full von-Kármán system studied in Yosibash et al. (2004). [2]

For the full and complete von-Kármán systems, filtering of the non-linear terms was employed to remove aliasing errors. The exponential filter $\sigma_E(\eta_n)$ (see Canuto et al. (1987)) given as follows was employed in each spatial direction:

$$\sigma_E(\eta) = \exp(-\alpha\eta^p) \tag{12}$$

where η is a parameter between $[0,1]$ which correlates to the polynomial order at which the filtering (dissipation) is being applied, where p denotes the order of the filter and where α is a scaling parameter (normally taken to be $\alpha = -\log(\epsilon_M)$ where $\epsilon_M = 10^{-14}$ is the standard machine zero). In this work, the order of

[2] The complete von-Kármán system differs from these studied in Yosibash et al. (2004) by the addition of the $\frac{-h^2}{12}\Delta w_{,tt}$ term. To accommodate the additional term, we modified our numerical scheme shown after Eq. (11) in Yosibash et al. (2004) as follows:

$$\left[\frac{4}{(\Delta t)^2}\left(\mathbf{I} - \frac{h^2}{12}\mathbf{D}_2\right) + c\frac{2}{\Delta t}\mathbf{I}\right]\vec{w}_{n+1} = \vec{g}_{n+1} + \left(\mathbf{I} - \frac{h^2}{12}\mathbf{D}_2\right)\left(\frac{4}{(\Delta t)^2}\vec{w}_n + \frac{4}{\Delta t}\dot{\vec{w}}_n + \ddot{\vec{w}}_n\right) + c\left(\frac{2}{\Delta t}\vec{w}_n + \dot{\vec{w}}_n\right)$$

where the subscripts n stand for the solution at time step n, $\mathbf{D}_2$ denotes the discretized version of the Laplacian operator, $\mathbf{I}$ denotes the identity operator, and $\vec{g}$ contains the bi-harmonic term and non-linear terms. The left-hand-side operator can be inverted directly so that one can solve the entire system using the fixed point method, as done in Yosibash et al. (2004).

Table 1
Constant loading on a non-damped plate: mid-point maximum difference in peak deflection and maximum relative phase difference for $0 < t < 15$ between the various von-Kármán models

von-Kármán models	$h = 0.1$	$h = 0.01$	$h = 0.001$
Peak deflection difference			
Complete-simplified	0.061565	0.021400	0.021164
Complete-full	0.051988	0.001842	0.001122
Full-simplified	0.024000	0.020575	0.020545
Relative phase difference			
Complete-simplified	0.1176	0.0484	0.0484
Complete-full	0.0986	0.0034	0.0034
Full-simplified	0.0484	0.0467	0.0467

the filter was taken to be $p = 4$ for all simulations. Filtering is necessary in the collocation approach due to the tacit interpolation projection which is accomplished when non-linear terms are handled point-wise. The non-linear products of polynomial solutions lies outside the original approximation space (dictated by the number of points used); interpolation projections allow aliasing errors to accumulate, and hence pollute the system. As shown in Yosibash et al. (2004), judicious use of filtering can minimize the influence of this afore-known (see e.g. Canuto et al. (1987)) numerical characteristic of using collocation methods for strongly non-linear problems.

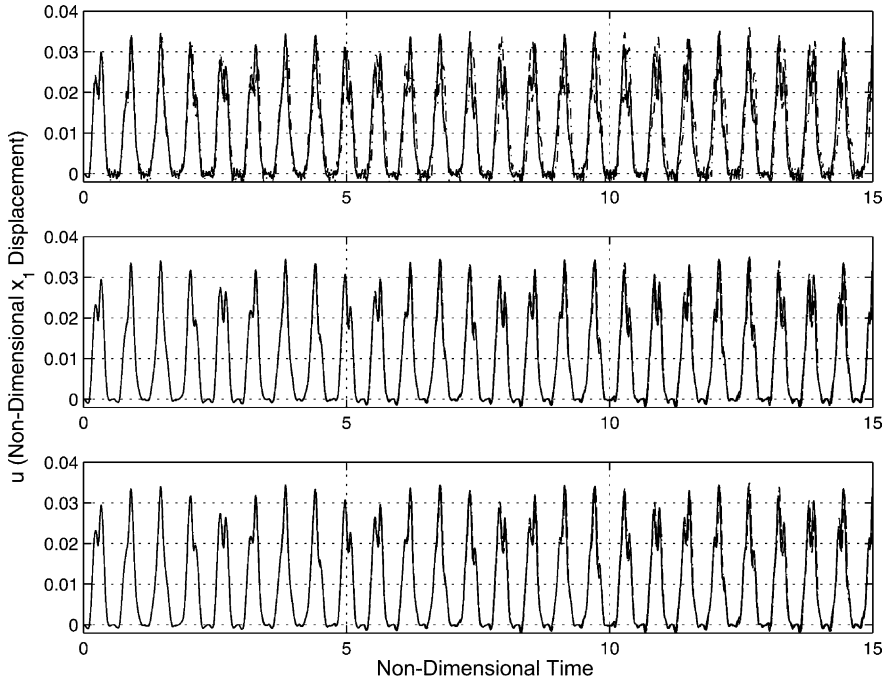

Fig. 4. Constant loading on a non-damped plate: $u(0.29, 0.29, 0 < t < 15)$ for the simplified (solid line), full (dashed line) and complete (dash-dot line) von-Kármán models. Upper $h = 0.1$, middle $h = 0.01$ and bottom $h = 0.001$ plate.

3. The difference in the various von-Kármán models response

Throughout the remaining of the paper we consider a $[0,2]\times[0,2]$ plate, clamped at its lateral boundaries, and having a Poisson ratio of $v = 0.3$. In all examples below it is expected that as the plate thickness h approaches zero, the three different von-Kármán models will converge to the same solution, as the difference between them is manifested in terms multiplying h^2.

As the deflection w is the data of interest in plates, we herein concentrate our attention on it.

3.1. Constant Heaviside loading on a non-damped plate

As the first example problem we consider a non-damped plate $c = 0$, subject to a Heaviside function representing a constant loading, i.e.

$$g_3 = \begin{cases} 0 & t < 0 \\ 29.6 & t \geqslant 0 \end{cases} \tag{13}$$

For this case the mid-side deflection $w(1,1,t)$ is an oscillating function of t, and due to the non-linearities, its amplitude is non-constant as a function of t.

In Fig. 2 we present the mid-point deflection $w(1,1,0 < t < 15)$ for three different plate thicknesses $h = 0.1,\ 0.01,\ 0.001$.

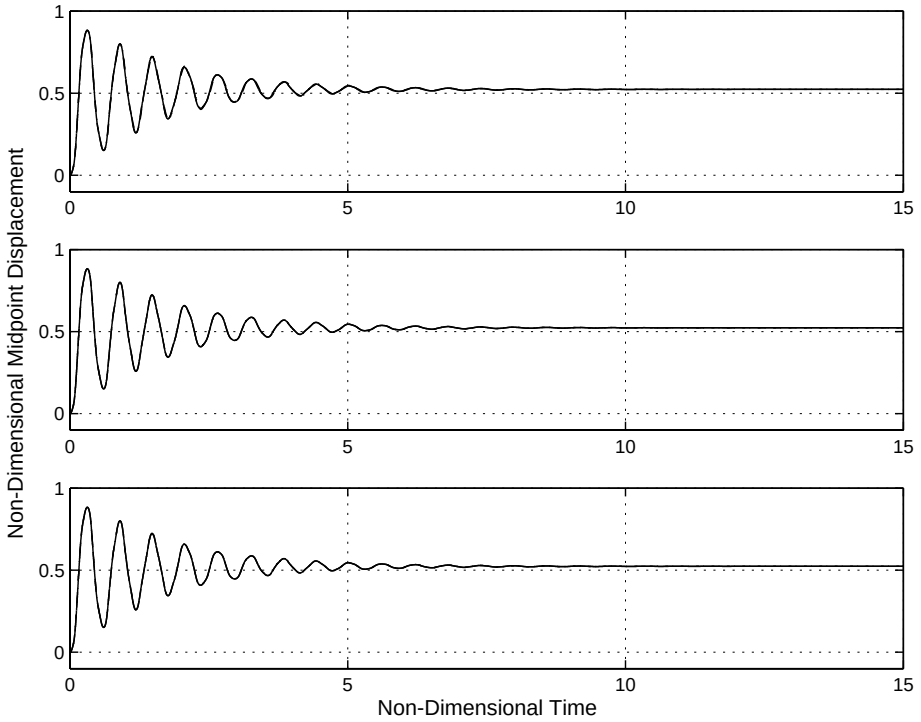

Fig. 5. Constant loading on a damped plate: mid-point deflection $w(1,1,t)$ for the simplified (solid line), full (dashed line) and complete (dash-dot line) von-Kármán models. Upper $h = 0.1$, middle $h = 0.01$ and bottom $h = 0.001$ plate.

Table 2
Constant loading on a damped plate: mid-point deflection at steady state ($t \approx 15$) for the various von-Kármán models

von-Kármán models	$h = 0.1$	$h = 0.01$	$h = 0.001$
Simplified	0.523088	0.523088	0.523088
Full	0.523234	0.523234	0.523234
Complete	0.523450	0.523000	0.523557

One may notice that indeed as $h \to 0$ the solutions of the three models converge to the same response. To better visualize the difference in the three different models, we present in Fig. 3 a zoomed view of the peak mid-point deflection occurring at $t \approx 8.5$.

We also summarize in Table 1 the maximum difference in the peaks, and the maximum relative difference in the phase (which is computed as the difference in time at the peak of two different models divided by the time of a cycle) for $0 < t < 15$. As the maximum peak is of an order of magnitude of 1 (i.e. the deflection is of the same order as the plate thickness), the difference in the peak values in Table 1 represents also the relative difference.

For $h = 0.1$ a relative difference of about 5–6% is visible between the complete and simplified models, and complete and full models, whereas a larger difference is visible in the phase shift between the two models. This indicates that the rotational inertia term has a smaller influence on the solution than the in-plane acceleration terms. However, for the smaller h values (0.01 and 0.001), the difference between the various models is considerably smaller (about 2% in peak values). Because of the filtering used to stabilized the numerical schemes for the complete and full models, a small difference of about maximum 2% remains as $h \to 0$ between these and the simplified model deflection (which does not use any filtering). Between the complete and full models the difference decreases considerably. This again indicates that the rotational inertia term has a small influence on the deflection response.

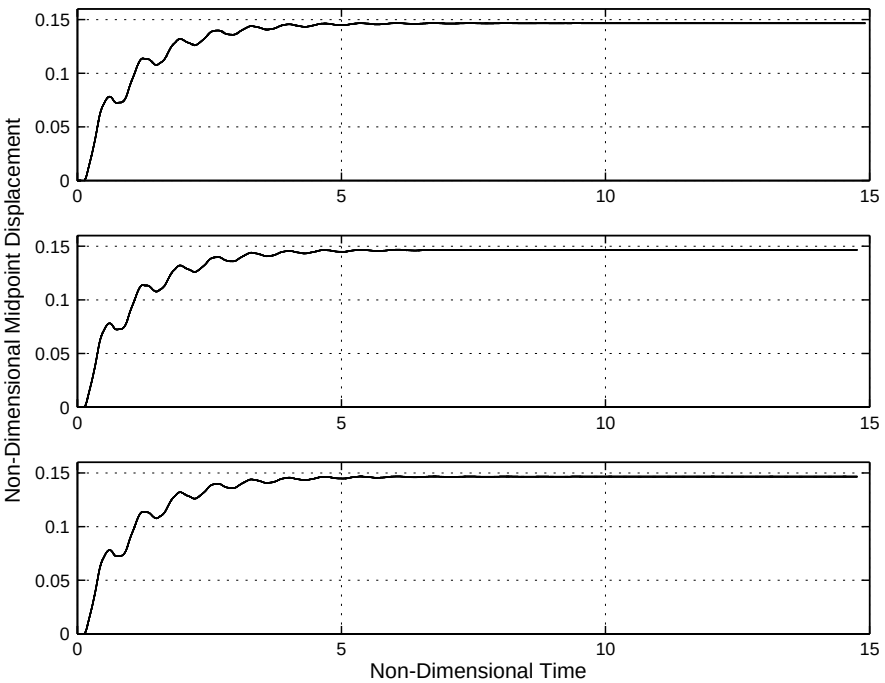

Fig. 6. Varying loading on a damped plate: mid-point deflection $w(1, 1, t)$ for the simplified (solid line), full (dashed line) and complete (dash-dot line) von-Kármán models. Upper $h = 0.1$, middle $h = 0.01$ and bottom $h = 0.001$ plate.

Table 3
Time varying loading on a damped plate: mid-point deflection at steady state ($t \approx 15$) for the various von-Kármán models

von-Kármán models	$h = 0.1$	$h = 0.01$	$h = 0.001$
Simplified	0.146586	0.146586	0.146586
Full	0.146633	0.146633	0.146633
Complete	0.146717	0.146530	0.146589

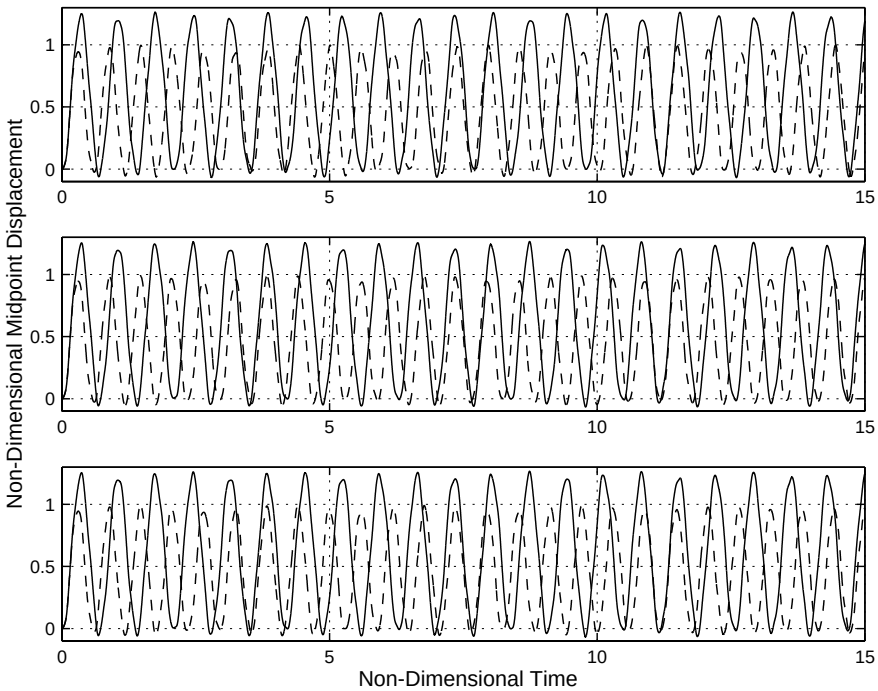

Fig. 7. Constant loading on a non-damped plate: mid-point deflection $w(1,1,t)$ for the Kirchhoff–Love model (14) (solid line) and the complete von-Kármán model (dashed line). Upper $h = 0.1$, middle $h = 0.01$ and bottom $h = 0.001$ plate.

Although the in-plane displacement components u and v are of marginal importance, and their magnitudes are smaller than the deflection w, we nevertheless present in Fig. 4 $u(0.29, 0.29, 0 < t < 15)$ (the offset point has been chosen since the mid-point is located at the intersection of the lines of symmetry for u and v). As the graph for $v(0.29, 0.29, 0 < t < 15)$ is almost identical as this shown for u, it is not presented. As for the deflection, for $h = 0.1$ a small difference is noticed between the various models, however this difference almost disappears for $h = 0.01$ and smaller. The in-plane displacement frequency is similar to the one observed for the deflection, but its amplitude is two orders of magnitude smaller compared to the deflection (although being inspected at a location shifted from the center, these orders of magnitude are visible throughout all plate locations).

3.2. Constant Heaviside loading on a damped plate

As the second example problem we consider a damped plate with $c = 1.25$, subject to a Heaviside function representing a constant loading as in Eq. (13). A decaying oscillatory mid-side deflection $w(1,1,t)$ is expected, with a steady state deflection being the same to all three von-Kármán models because the terms

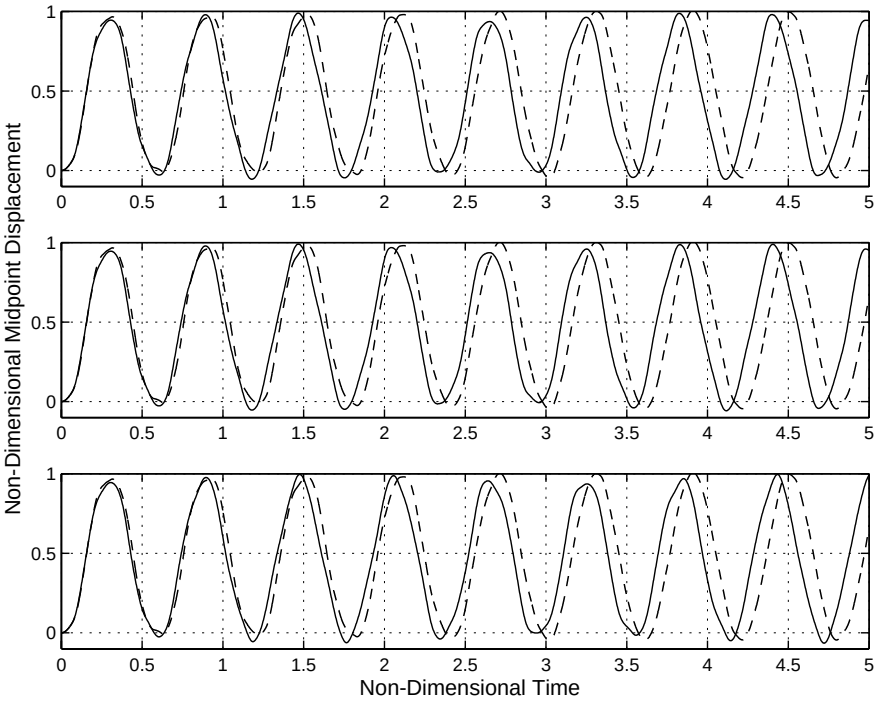

Fig. 8. Constant loading on a non-damped plate: mid-point deflection $w(1,1,t)$ for the simplified von-Kármán model and 3-D plate (upper), full von-Kármán model and 3-D plate (middle) and complete von-Kármán model and 3-D plate (bottom). Plate thickness is $h = 0.1$.

multiplying the thickness dependent term vanish at the steady state. In Fig. 5 we present the mid-point deflection $w(1,1,0 < t < 15)$ for three different plate thicknesses $h = 0.1,\ 0.01,\ 0.001$.

In this example problem one may notice the negligible difference between the three different solutions. In Table 2 we present the mid-point deflection at the steady state, defined as $w(1,1,t \approx 15)$, for the three von-Kármán models at the three thicknesses. All models at all thicknesses indeed converge to the same value which is identical up to three significant digits.

3.3. A time varying loading on a damped plate

The third example problem represents a damped plate with $c = 1.25$, subject to a Heaviside time-varying function which tends to a constant loading as $t \to \infty$:

$$g_3 = \begin{cases} 0 & t < 0 \\ 118.4(1 - \mathrm{e}^{-t})\cos^2(\pi x/2)\cos^2(\pi y/2) & t \geqslant 0 \end{cases}$$

This example problem is considered so to investigate the three different von-Kármán models under a time-varying loading. Fig. 6 presents the mid-point deflection $w(1,1,0 < t < 15)$ for the three different plate thicknesses $h = 0.1,\ 0.01,\ 0.001$.

In Table 3 we present the mid-point deflection at the steady state, defined as $w(1,1,t \approx 15)$, for the three von-Kármán models at the three thicknesses. All models at all thicknesses indeed converge to the same value which is identical up to three significant digits.

3.4. The linearized model—Kirchhoff–Love plate model

By removing the non-linear terms in the complete von-Kármán plate model ((7)–(9)), a model similar to the well-known Kirchhoff–Love plate model [3] is obtained, which reads:

$$w_{,tt} + cw_{,t} - \frac{h^2}{12}\Delta w_{,tt} + \Delta^2 w = g_3 \tag{14}$$

$$\frac{h^2}{6}(u_{,tt} + cu_{,t}) - [2u_{,11} + (1+\nu)v_{,12} + (1-\nu)u_{,22}] = 0 \tag{15}$$

$$\frac{h^2}{6}(v_{,tt} + cv_{,t}) - [2v_{,22} + (1+\nu)u_{,12} + (1-\nu)v_{,11}] = 0 \tag{16}$$

Because Eq. (14) for w is completely decoupled from these for u, v (Eqs. (15) and (16)), one can solve (14) alone. Although it is well-known that the static von-Kármán solution and the Kirchhoff–Love solution differ considerably for large deflections, (when the deflection is of the same order of magnitude as the plate thickness), we herein compare their solutions in Fig. 7, for the clamped non-damped plate ($c = 0$) under the constant loading in Eq. (13). Not only that there is a considerable difference in the amplitude of oscillations (and because of the in-plane tension the deflection amplitude is smaller by more than 30% for the von-Kármán model), but a considerable phase difference is visible too, as expected.

4. Modeling errors: difference between the three-dimensional and von-Kármán models

To quantify the modeling error, we constructed a three-dimensional finite element model, using the finite element commercial code ADINA™. [4] A quarter of the plate has been modeled, with $30 \times 30 \times 2$ 20-node hexahedral finite elements (two elements in the thickness direction). Because physical quantities are used in ADINA, we chose $E^* = 100$, $\rho^* = 10$, and the time-step for the implicit time marching algorithm was taken to be $\Delta t^* \approx 10^{-4}$ for the plate of thickness $h^* = 0.1$ and $\Delta t^* \approx 10^{-5}$ for the plate of thickness $h^* = 0.01$. We considered a non-damped plate thus $c^* = 0$. The plate has been loaded by the Heaviside constant loading described in Eq. (13). We performed also additional analyses with a $20 \times 20 \times 2$ mesh and a time step 2.5 times larger to ensure that the numerical errors in the finite element analysis are small. We present in Figs. 8 and 9 the non-dimensionalized mid-point deflection for the 3-D plate of thickness $h = 0.1$ and $h = 0.01$ (in the middle of the plate in the thickness-wise direction) compared to the various von-Kármán plate models.

To better quantify the differences between the three-dimensional plate mid-point deflection and the three von-Kármán models we summarize in Table 4 the normalized max difference in peak deflection and maximum relative phase difference for $0 < t < 5$.

For the $h = 0.1$ plate, the difference in the maximum mid-point deflection between the 3-D model and *all* von-Kármán plate models is of an order of magnitude of 7%, and reduces to 1–2% for the $h = 0.01$ plate. Therefore, neglecting the rotational inertia term in the equation for w and the inertia terms in the equations for u,v, thus simplifying the von-Kármán plate model considerably, is a far less important idealization error compared to the dimensional reduction idealization errors introduced when deriving the von-Kármán plate model. This suggests that using the simplified von-Kármán plate model (which is considerably simpler from numerical viewpoint) is fully justified as far as idealization errors are concerned, and the complete or full von-Kármán models provide no advantage.

[3] The classical Kirchhoff–Love plate model is obtained by considering (14) alone and taking $h = 0$ so that the third term vanishes. For further details the reader is referred to Reismann (1998, Chap. 6).

[4] Adina is a TradeMark of ADINA R&D, Inc., 71 Elton Avenue Watertown, MA 02472, USA.

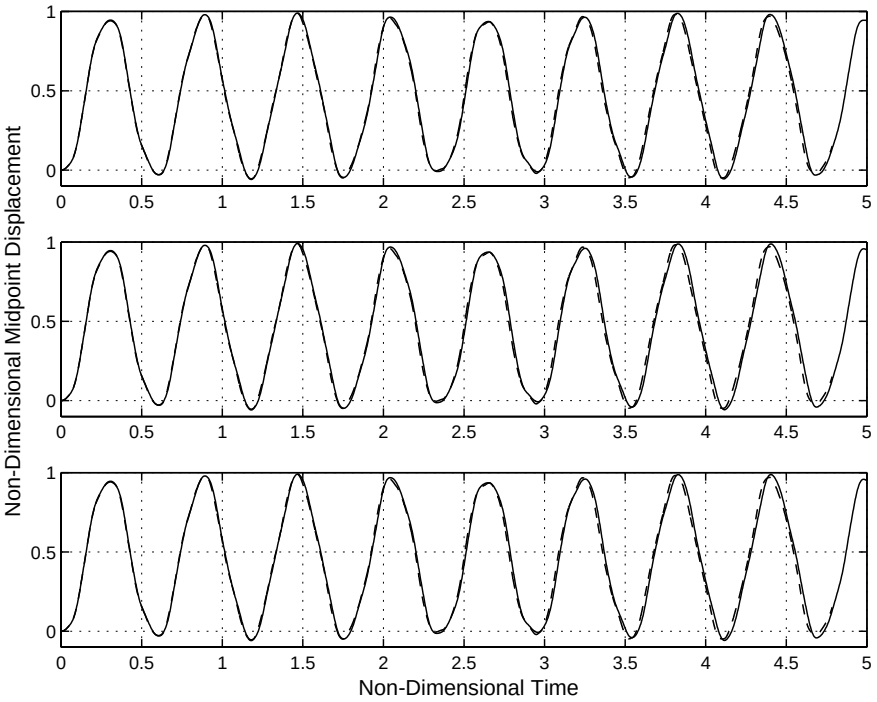

Fig. 9. Constant loading on a non-damped plate: mid-point deflection $w(1,1,t)$ for the simplified von-Kármán model and 3-D plate (upper), full von-Kármán model and 3-D plate (middle) and complete von-Kármán model and 3-D plate (bottom). Plate thickness is $h = 0.01$.

Table 4
Mid-point max difference in peak deflection and maximum relative phase difference for $0 < t < 5$ between the 3-D plate and von-Kármán models

von-Kármán models	$h = 0.1$	$h = 0.01$
Peak deflection difference		
3D-simplified	0.071775	0.011289
3D-full	0.072107	0.018026
3D-complete	0.070156	0.018154
Relative phase difference		
3D-simplified	0.17053	0.02369
3D-full	0.16185	0.02888
3D-complete	0.12630	0.02715

5. Summary and conclusions

The complete dynamic von-Kármán system is a set of three coupled non-linear PDEs involving a bi-harmonic operator, a Laplace operator on acceleration terms and first and second time derivatives. As all prior publications addressing the von-Kármán plate models (which we are aware of) neglect a-priori several terms in the system of equations, because of being considerably smaller compared to the other terms, it was our aim in this paper to quantify the errors associated with these assumptions.

Herein three various dynamic von-Kármán plate models have been investigated, and the difference in these are documented. Specifically, we consider the *complete* model in which we retained all terms in the system of equations (this model has not yet been investigated elsewhere), one named *full* in which the rotational inertial term in the equation of the transverse deflection has been removed, and the *simplified* model (which is the most common model used in past literature) in which another two terms in the equations for in-plane displacements, representing in-plane inertial terms have been removed. These terms are removed as they are of an order h^2 compared to the other order 1 terms. Our analysis considers a model problem of a square plate with hard clamped boundary conditions.

As has been shown, the dynamic response of the various models is very similar, and neglecting the inertial terms, as frequently done in the literature, does not affect much the deflection (w, the function which is of most interest in plates). The differences, however, between the dynamic response of the various von-Kármán models and the three-dimensional model is considerably larger for plates considered moderately thin ($h/a = 1/20$), both in amplitude and phase difference. As $h/a \to 0$, for example for $h/a = 1/200$, this difference has been shown to be very small.

One other important observation is that the von-Kármán and Kirchhoff–Love plate models yield different responses both in amplitude and phase, for any h/a ratio.

Acknowledgments

Special thanks are extended to Dr. Mordechai Szanto from Rotem Industries, Israel for his assistance with the Adina code in performing the 3-D plate analyses, and to Prof. Irena Lasieka of the Department of Mathematics at University of Virginia, VA, USA, for helpful discussions and important remarks.

The second author gratefully acknowledges the computational support and resources provided by the Scientific Computing and Imaging Institute at the University of Utah.

References

Canuto, C., Hussaini, M., Quarteroni, A., Zang, T., 1987. Spectral Methods in Fluid Mechanics. Springer-Verlag, New York.

Chia, C.-Y., 1980. Nonlinear analysis of plates. McGraw-Hill.

Ciarlet, P.G., 1990. Plates and Junctions in Elastic Multi-Structures. An Asymptotic Analysis. RMA 14. Masson/Springer-Verlag.

Gordnier, R., Fithen, R., 2001. Coupling of a nonlinear finite element structural method with Navier–Stokes solver. AIAA 2001-2853. In: 31st Fluid Dynamics Conference, June 2001.

Gordnier, R., Visbal, M., 2002. Development of a three-dimensional viscous aeroelastic solver for nonlinear panel flutter. J. Fluids Struct. 16, 497–527.

Han, W., Petyt, M., 1997. Geometrically nonlinear vibration analysis of thin, rectangular plates using the hierarchical finite element method—I: The fundamental mode of isotropic plates. Comp. Struct. 63, 295–308.

Humar, J., 2002. Dynamics of Structures. A.A. Balkema Publishers.

Kirby, R., Yosibash, Z., 2004. Solution of von-Kármán dynamic non-linear plate equations using a pseudo-spectral method. Comp. Meth. Appl. Mech .Eng. 193 (6-8), 575–599.

Koch, H., Lasiecka, I., 2002. Hadamard well-posedness of weak solutions in nonlinear dynamic elasticity-full von Karman systems. Progress Nonlinear Diff. Eqs. 50, 197–216.

Lagnese, J.E., 1989. Boundary Stabilization of Thin Plates. SIAM.

Lasiecka, I., 1998. Uniform stabilizability of a full von Karman system with nonlinear boundary feedback. SIAM J. Control Optim. 36 (4), 1376–1422.

Nath, Y., Kumar, S., 1995. Chebyshev series solution to non-linear boundary value problems in rectangular domain. Comp. Meth. Appl. Mech. Eng. 125, 41–52.

Reismann, H., 1998. Elastic Plates: Theory and Application. John Wiley and Sons.

Trefethen, L.N., 2000. Spectral Methods in Matlab. SIAM.

Yosibash, Z., Kirby, R., Gottlieb, D., 2004. Pseudo-spectral methods for the solution of the von-Kármán dynamic non-linear plate system. J. Comp. Phys. 200, 432–461.